COMPARISON BETWEEN GNSS AND RADIOSOUNDING INTEGRATED WATER VAPOR AT GRUAN'S NY-ALESUND STATION

Javier VAQUERO-MARTÍNEZ[1,2], Manuel ANTÓN[1,2], José Pablo ORTIZ DE GALISTEO[3,4], Victoria E. CACHORRO[3], David MATEOS[3], Roberto ROMÁN[3]
[1]*Departamento de Física, Universidad de Extremadura.*
[2]*Grupo de Óptica Atmosférica. Universidad de Valladolid.*
[3]*Agencia Estatal de Meteorología.*
javier_vm@unex.ex, **mananton@unex.es**, **jortizd@aemet.es** , **chiqui@goa.uva.es** , **mateos@goa.uva.es** , **robertor@goa.uva.es**

RESUMEN
La observación del vapor de agua es un desafía de gran importancia, debido a que este es fundamental en el sistema climático. A pesar de la variedad de instrumentos que miden el vapor de agua, su alta variabilidad en los dominios temporal y espacial hace difícil dar mediciones completas. Las radiosondas (RS) permiten obtener el perfil vertical del vapor de agua, y están consolidadas como referencia. En las últimas décadas, los sistemas satelitales de navegación global (GNSS) proporcionan medidas de vapor de agua integrado (IWV), y se están implementando redes densas de receptores se están implementando gracias a su bajo coste, alta tasa de medidas, y su uso para otras aplicaciones en geofísica. Ambos instrumentos se compararon en la estación de Ny-Alesund, perteneciente a la red GRUAN, siendo RS la referencia, con un alto grado de correlación y un pequeño error sistemático (alrededor de 0.7 mm). Sin embargo, se observaron algunas dependencias: se han estudiado las dependencias con IWV, ángulo solar cenital (SZA) y presión en superficie. Un aumento en IWV lleva a un descenso del error medio (MBE) relativo, y de la desviación estándar (SD) relativa, mientras que los aumentos del SZA y la presión también empeoran el MBE, mientras que la SD se mantiene estable.

Palabras clave: vapor de agua, GNSS, Radiosondeo, Ny-Alesund, ártico.

ABSTRACT
Monitoring water vapor is a challenge of great importance because of its fundamental character in the climate system. Despite the variety of instruments to measure water vapor, its high variability in the spatial and temporal regimes makes it difficult to provide complete measurements. Radiosondes (RS) allow to retrieve the vertical profile of water vapor, and are consolidated as a reference. In the last decades, Global Navigation Satellite Systems (GNSS) provide integrated water vapor (IWV) measurements, and dense networks of receivers are being implemented because of their low cost, high measurement rate and use in other geophysics applications. Both instruments in Ny-Alesund GRUAN station are compared, being RS the reference, with a high degree of correlation, and a small, dry bias (around 0.7 mm). Nevertheless, some dependences are observed: IWV, solar zenith angle and

surface pressure are studied. Increase in IWV lead to lower relative mean biased error (MBE, in %) and standard deviation (SD), while SZA and pressure increases also worsens both MBE, while SD is quite stable.

Key words: water vapor, GNSS, radiosounding, Ny-Alesund, Arctic.

RESUMEN

La observación del vapor de agua es un desafío de gran importancia, debido a que este es fundamental en el sistema climático. A pesar de la variedad de instrumentos que miden el vapor de agua, su alta variabilidad en los dominios temporal y espacial hace difícil dar mediciones completas. Las radiosondas (RS) permiten obtener el perfil vertical del vapor de agua, y están consolidadas como referencia. En las últimas décadas, los sistemas satelitales de navegación global (GNSS) proporcionan medidas de vapor de agua integrado (IWV), y se están implementando redes densas de receptores se están implementando gracias a su bajo coste, alta tasa de medidas, y su uso para otras aplicaciones en geofísica. Ambos instrumentos se compararon en la estación de Ny-Alesund, perteneciente a la red GRUAN, siendo RS la referencia, con un alto grado de correlación y un pequeño error sistemático (alrededor de 0.7 mm). Sin embargo, se observaron algunas dependencias: se han estudiado las dependencias con IWV, ángulo solar cenital (SZA) y presión en superficie. Un aumento en IWV lleva a un descenso del error medio (MBE) relativo, y de la desviación estándar (SD) relativa, mientras que los aumentos del SZA y la presión también empeoran el MBE, mientras que la SD se mantiene estable.

Palabras clave: vapor de agua, GNSS, Radiosondeo, Ny-Alesund, ártico.

1. INTRODUCTION

Despite the low concentration of water vapor in the atmosphere, it has a paramount importance in the climate system, as it is acknowledged as the most important atmospheric greenhouse gas. Although it is not directly involved in global warming, it causes a positive feedback on the climate system (Colman, 2003; Colman, 2015).

However, in order to understand the effects of water vapor on climate, it is necessary to retrieve quality water vapor data. The main problem is the high variability of this gas, both in the temporal and spatial domains.

The Integrated Water Vapor (IWV) is the variable commonly used to study the atmospheric water vapor. IWV is a magnitude equivalent to condensing all the water vapor in the atmospheric vertical column and measuring the height that it would reach if contained in a vessel of unit cross section, being its units superficial density (g mm^{-2}) or length (mm).

This variable can be measured by radiosounding (RS), one of the most precise and direct methods to measure water vapor profiles, and used commonly to validate other instruments (Antón, et al., 2015; du Piesanie et al., 2013; Ohtani & Naito, 2000). However they are quite limited in the temporal (generally 1-2 measurements per day) and spatial domains. Global Navigation Satellite Systems (GNSS) can be

used to derive IWV data as well (Bevis et al., 1992). They are not as precise as RS, but they have some advantages: all-weather availability, high temporal resolution (5 min to 2 hourly), high accuracy (less than 3 mm in IWV) and long-term stability.
Ny-Alesund station is part of the Global Climate Observing System (GCOS) Reference Upper-Air Network (GRUAN), which has recognized the need of having redundant water vapor measurements in order to improve their quality (GRUAN, 2007). The main goal of this study is to compare the IWV from GNSS against IWV from RS at this station, which of special interest for its location, in the Arctic.

2. DATA AND METHODOLOGY

2.1. IWV from GRUAN GNSS product

GNSS can be used to obtain IWV measurements with an hourly temporal resolution. The method is described in Bevis et al. (1992). The communication between GNSS satellite and receiver through microwaves takes some time, and such time is used to calculate the distance between satellite and receiver. The distances to several satellites allows to triangulate the position of the receiver. However, in its travel throughout the atmosphere the signal suffers some delays. The slant tropospheric delay (STD) is caused by the troposphere, and it can be seen as the sum of two terms: first, the slant hydrostatic delay (SHD) and second, the slant wet delay (SWD). The former is caused by all the gases in the atmosphere, and can be estimated by a simple model (Saastamoinen, 1972) of which the only inputs are surface pressure and latitude, while the former is caused by the water vapor alone. Mapping functions (Boehm et al., 2006; Niell, 2000) can be applied in order to obtain the zenithal equivalent of these amounts, zenith tropospheric delay (ZTD), zenith hydrostatic delay (ZHD) and zenith wet delay (ZWD). ZWD can therefore be measured from the difference of ZTD (obtained by GNSS processing) and ZHD (obtained by Saastamoinen model), and it can be converted to IWV.
GRUAN provides both ZTD and IWV products for those stations equipped for GNSS. At Ny-Alesund there are three stations: *nya1*, *nya2*, and nyal. However, IWV data is only available for *nya1*.

2.2. IWV from GRUAN RS product

GRUAN provides radiosonde data for 28 sites. Ny-Alesund's site identification is NYA. RS and GNSS GRUAN data at Ny-Alesund are coincident in the period from 05/15/2007 to 01/10/2018. Radiosonde launches are typically at 12h but there are launches at other hours, especially at 00, 06 and 18h.
The sondes used at this station are Vaisala RS92. The RS92 model is equipped with a wire-like capacitive temperature sensor (*thermocap*), a silicon-based pressure detector and a GPS receiver. More detailed information about the processing of RS data can be found at https://www.gruan.org/instruments/radiosondes/sonde-models/vaisala-rs92/ or (Dirksen et al., 2014). The main error sources that affect the humidity sensor are: daytime solar heating of humicaps (dry bias), sensor time-lag at temperatures below -40º, and temperature-dependent calibration correction.

The GRUAN RS92 product includes a wide variety of profiles, such as pressure, temperature, humidity, relative humidity, water vapor mixing ratio (WVMR), winds, frostpoint, short-wave radiation and associated uncertainties. IWV can be calculated directly by integration of water vapor mixing ratio (WVMR) in pressures. In addition, some restrictions were considered in order to ensure data quality: the number of levels must be higher than 15; the first level must be below 1 km height and the last level must be above 9 km height; the resulting values of IWV must make sense (IWV positive and smaller than 100 mm).

2.3. Methodology

The criterion to match GNSS and RS required that time differences between RS launch and GNSS measurement had to be below 30 minutes. RS measurement were considered as references and two variables were analyzed: the physical difference (GNSS minus RS) and relative differences (physical difference divided by RS value and multiplied by 100%). The mean of differences (also known as mean bias error, MBE), and the standard deviation of the differences (SD) were calculated. The former is a measurement of accuracy and the latter, of precision.

Data was divided into bins of several variables in order to study the precision and accuracy in each bin, and determine the possible dependencies on these variables. Bins with less than 15 data were rejected, as they are not representative.

3. RESULTS

3.1. Overall statistics and regressions.

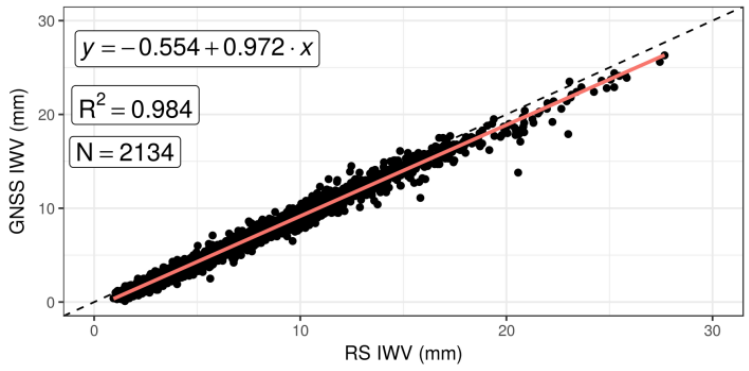

Fig. 1: Scatter-plot of GNSS and RS IWV products. Black dashed line represents the identity line and red full line represents the linear fit.

Fig. 1 shows the scatterplot of GNSS and RS IWV data. R^2 shows a high degree of linear correlation and regression line shows that GNSS tends to underestimate IWV when compared to RS.

The slope of 0.972 is a bit below the ideal 1.000. Other statistics have been computed as well: MBE is -0.78 mm, median -0.75 mm and SD is 0.62 mm.

3.2. Dependence of GNSS-RS difference on IWV.

The available data-set was divided into bins of 5 mm. MBE and SD were computed for relative differences, as shown in Fig. 2 and Fig. 3, respectively. MBE clearly worsens (more negative) at IWV below 10 mm, while between 10 and 25 mm it keeps a rather stable value, around -6 %. However, absolute MBE (in mm, computed by physical differences, and not shown in this text) has a constant value around -0.7 mm between 0 and 15 mm, becoming more negative as IWV increases from 15 mm to 25 mm, reaching values below -1.5 mm.

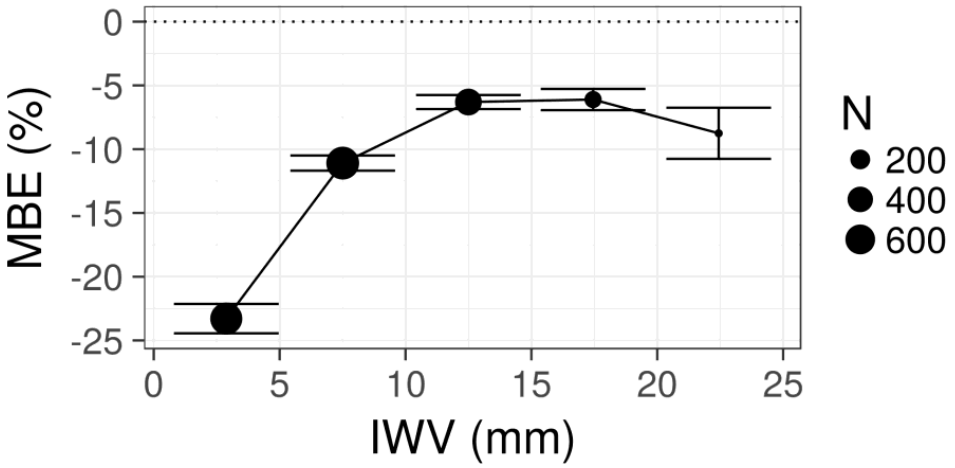

Fig. 2: MBE of GNSS-RS relative differences along RS IWV values.

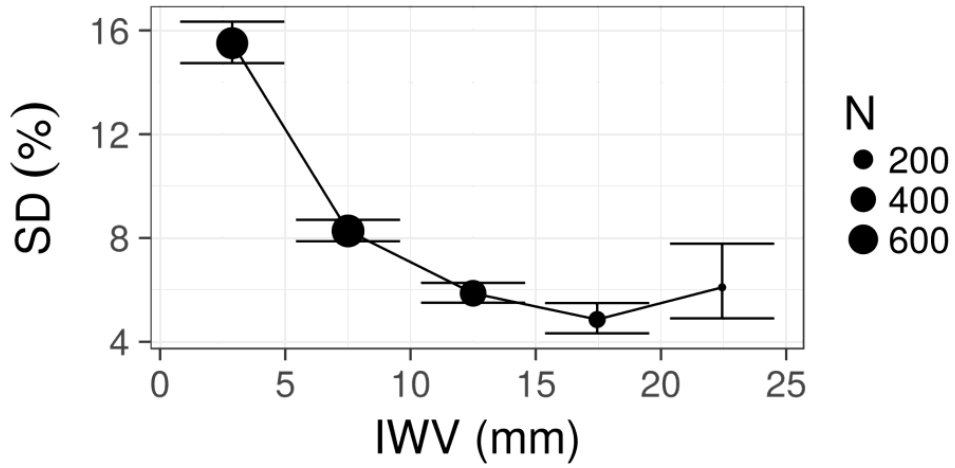

Fig. 3: SD of GNSS-RS relative differences on RS IWV values

SD presents a rather similar behaviour. Values below 10 mm increase SD at decreasing IWV, while those above 10 mm show a rather constant value, around 6%. For physical differences (not shown), SD increases monotonously with increasing IWV, from 0.4 mm up to 1.3 mm.

3.3. Dependence of GNSS-RS difference on SZA.

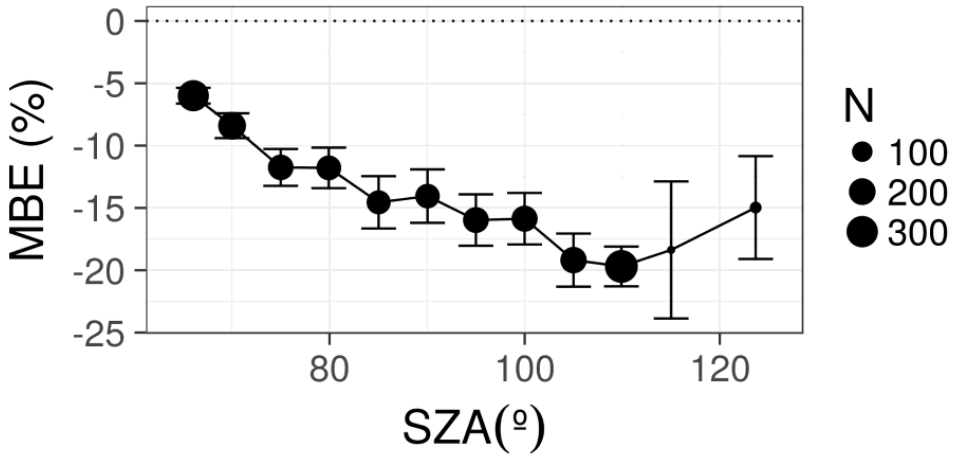

Fig. 4: MBE of GNSS-RS relative differences (%) with respect to SZA.

The evolution of MBE of relative differences with SZA is shown in Fig. 4. MBE decreases (higher differences without sign) as SZA increases. For values above 90º MBE is approximately constant, slightly above -20%. However, MBE in mm (calculated from physical differences, not shown), exhibits a rather stable value around -0.75 mm.

The SD from relative differences is presented in Fig. 5. Again, no significant differences arise for values above 90º, with SD around 14%. Below 90º, however, SD exhibits a clear increase with SZA. SD from physical differences, however, shows a stable value around 0.6 mm, except for the 65º bin with 0.8 mm and the 110º bin, with a SD below 0.5.

MBE (%) variation with pressure exhibited, as shown in Figure 7, is stable around -13% up to 1000hPa, where MBE decreases with pressure up to -20% for 1027.5 hPa bin. A similar behaviour is observed for MBE in mm, with approximately constant values around -0.74 mm, up to 1000 hPa. From 1000 hPa upwards, MBE decreases with pressure, reaching values below -1.00 mm at 1027.5 hPa.

SD (%) variation with respect to pressure values is shown in Fig. 7. There is an increasing tendency as pressure increases. However, between 990 and 115 hPa values are quite stable, around 13%. The SD for physical differences also has stable values, around 0.6 mm, except for the last bin (1025-1030 hPa), which is below 0.4 mm.

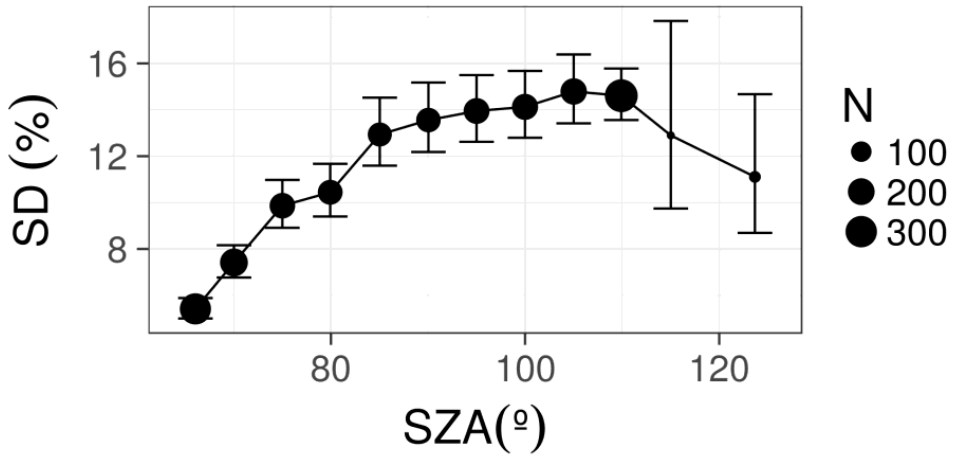

Fig. 5: SD of GNSS-RS differences (%) with respect to SZA

3.4. Dependence of GNSS-RS difference on pressure.

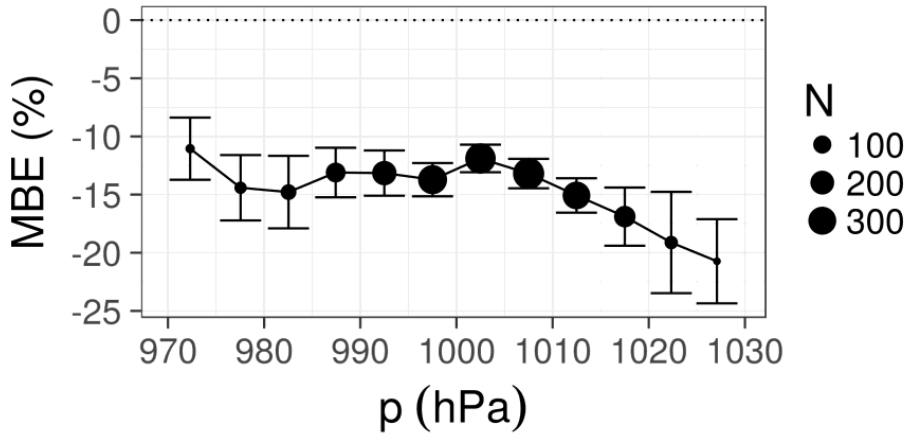

Fig. 6: MBE of GNSS-RS differences (%) with respect to pressure

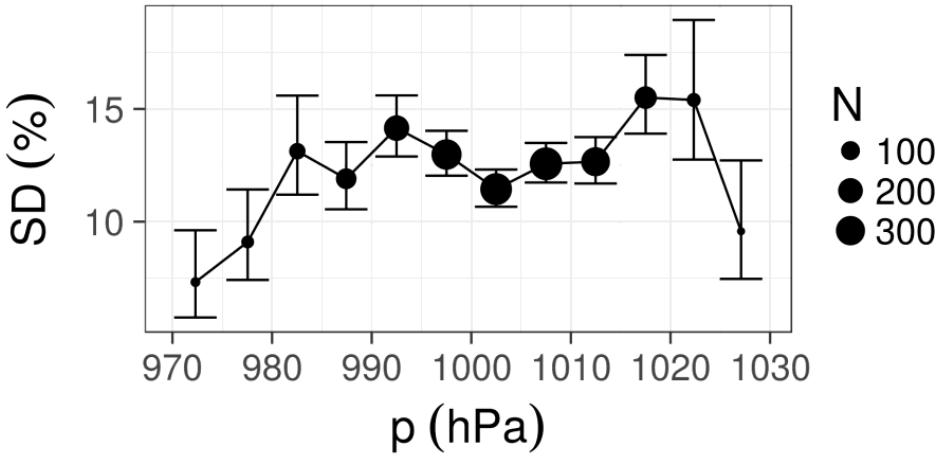

Fig. 7: SD of GNSS-RS differences (%) with respect to pressure

4. DISCUSSION AND CONCLUSIONS

4.1. Overall statistics and regressions.

The agreement between GNSS and RS data has a high degree of correlation, which indicates that differences are not generally important. It is shown that GNSS tend to underestimate IWV with respect to RS. Hordyniec et al. (2015) indicated that GNSS IWV retrievals suffer from biases of at least 0.5 mm, which is in agreement with the observations in this work.

4.2. Dependence of GNSS-RS difference on IWV.

The physical differences between GNSS-RS are shown to increase (in absolute value) as IWV increase. However, such increase is small, around 1.5 mm in the whole range of IWV (0-25 mm). Therefore, the relative differences tend to get closer to zero with IWV. The same reasoning can be applied to SD values. This is expected because higher RS IWV values are associated with higher RS IWV uncertainties.

4.3. Dependence of GNSS-RS difference on SZA.

SZA related differences could be due to errors in radiosonde sensors (especially humidity sensor, which is affected by solar radiation), as stated in Dirksen et al. (2014) and Wang & Zhang (2008). However, physical differences did not show such evolution, while relative differences show the opposite behaviour (higher dry bias at high SZA, when less solar radiation is present), which could be due to compensation of GNSS and RS biases. Typical IWV values at those SZA bins can also influence the results, and explain SD behaviour, since at low SZA IWV is generally higher, with lower relative SD.

4.4. Dependence of GNSS-RS difference on pressure.

The observed dependences on pressure could be related to the errors associated to ZHD estimation through the Saastamoinen model, which uses surface pressure as input, and also to the typical values of IWV along the different pressure bins.

4.5. General conclusions

From this work it can be concluded that GNSS and RS agree well, and GNSS can certainly be used as a reference for validation of other instruments with its advantages over RS, like much higher

ACKNOWLEDGMENTS

Support from the Junta de Extremadura (Research Group Grants GR15137) is gratefully acknowledged. Work at Universidad de Valladolid is supported by project CMT2015-66742-R. The authors wish to thank the operators of Ny-Alesund observatory for dutifully performing reference radiosoundings and maintenance of RS and GNSS according the GRUAN standards, as well as GFZ Helmholtz Center Potsdam for their processing of GNS data products to obtain ZTD and IWV, and acknowledge ERA-Interim data.

REFERENCES

Antón, M., Loyola, D., Román, R., & Vömel, H. (2015). Validation of GOME-2/MetOp-A total water vapour column using reference radiosonde data from the GRUAN network. *Atmospheric Measurement Techniques*, *8*(3), 1135–1145. https://doi.org/10.5194/amt-8-1135-2015

Bevis, M., Businger, S., Herring, T. A., Rocken, C., Anthes, R. A., & Ware, R. H. (1992). GPS Meteorology: Remote Sensing of Atmospheric Water Vapor Using the Global Positioning System. *Journal of Geophysical Research*, *97*(D14), 15787–15801. https://doi.org/10.1029/92JD01517

Boehm, J., Niell, A., Tregoning, P., & Schuh, H. (2006). Global Mapping Function (GMF): A new empirical mapping function based on numerical weather model data. *Geophysical Research Letters*, *33*(7), 3–6. https://doi.org/10.1029/2005GL025546

Colman, R. (2003). A comparison of climate feedbacks in general circulation models. *Climate Dynamics*, *20*, 865–873. https://doi.org/10.1007/s00382-003-0310-z

Colman, R. A. (2015). Climate radiative feedbacks and adjustments at the Earth's surface. *Journal of Geophysical Research: Atmospheres*, *120*(8), 3173–3182. https://doi.org/10.1002/2014JD022896

Dirksen, R. J., Sommer, M., Immler, F. J., Hurst, D. F., Kivi, R., & Vömel, H. (2014). Reference quality upper-air measurements: GRUAN data processing for the Vaisala RS92 radiosonde. *Atmospheric Measurement Techniques*, *7*(12), 4463–4490. https://doi.org/10.5194/amt-7-4463-2014

du Piesanie, A., Piters, A. J. M., Aben, I., Schrijver, H., Wang, P., & Noël, S. (2013). Validation of two independent retrievals of SCIAMACHY water

vapour columns using radiosonde data. *Atmospheric Measurement Techniques*, *6*(10), 2925–2940. https://doi.org/10.5194/amt-6-2925-2013

GRUAN. (2007). *Justification, requirements, siting, and instrumentation options* (Report). (WMO, Ed.) (p. 44). GRUAN Lead Centre, DWD. Retrieved from https://www.gruan.org/gruan/editor/documents/gcos/gcos-112.pdf

Hordyniec, P., Bosy, J., & Rohm, W. (2015). Assessment of errors in Precipitable Water data derived from Global Navigation Satellite System observations. *Journal of Atmospheric and Solar-Terrestrial Physics*, *129*, 69–77. https://doi.org/10.1016/j.jastp.2015.04.012

Niell, A. E. (2000). Improved atmospheric mapping functions for VLBI and GPS. *Earth, Planets and Space*, *52*(10), 699–702. https://doi.org/10.1186/BF03352267

Ohtani, R., & Naito, I. (2000). Comparisons of GPS-derived precipitable water vapors with radiosonde observations in Japan. *Journal of Geophysical Research: Atmospheres*, *105*(D22), 26917–26929. https://doi.org/10.1029/2000JD900362

Saastamoinen, J. (1972). Atmospheric Correction for the Troposphere and Stratosphere in Radio Ranging Satellites. In: S. W. Henriksen, A. Mancini, & B. H. Chovitz (Eds.), *Geophysical Monograph Series* (pp. 247–251). Washington, D. C.: American Geophysical Union. https://doi.org/10.1029/GM015p0247

Wang, J., & Zhang, L. (2008). Systematic Errors in Global Radiosonde Precipitable Water Data from Comparisons with Ground-Based GPS Measurements. *Journal of Climate*, *21*(10), 2218–2238. https://doi.org/10.1175/2007JCLI1944.1